STRUCTURAL, MAGNETIC AND ELECTRICAL BEHAVIOUR OF SR-HEXAFERRITE BY SUBSTITUTION OF Co AND Zr BY SOL-GEL METHOD

C.L. Khobaragade[@], S.V. Soni[#], A.K. Akant[$], R. Khatarkar[#], U. Rathod[&], K. G. Rewatkar[q]

[@]Deptt. of Applied Physics, Govindrao Wanjari College of Engg. & Tech., Nagpur, India

[#] Deptt. of Applied Physics, Yashwantrao Chavan College of Engg., Nagpur, India

[$]Deptt. of Applied Physics, Manoharbhai Patel College of Engg., Gondia, India

[&]Deptt. of Applied Physics, Dr. Ambedkar College of Engg. & Research Institute, Nagpur, India

[q]Deptt. of Physics, Dr. Ambedkar College, Deeksha Bhoomi, Nagpur, India

Mobile: +919823343628 E-mail: chanduparulk@gmail.com

Abstract:

M-type hexaferrites $SrFe_{12-2x-y}(CoZr)_xO_{19}$ (x = 0.2, 0.6, 0.8, 1.0) powders are synthesized by using sol-gel combustion method in nitrate citric acid systems. The X-ray diffraction pattern at room temperature shows that the prepared samples have a single phase and the effect of composition on the unit cell parameters, density and porosity has been studied. The X-ray diffraction patterns of $SrFe_{12-2x-y}(CoZr)_xO_{19}$ annealed at 750℃ manifest that all the species have hexagonal crystal structure with lattice constants of a = 5.80 - 5.86 Å and c = 22.08 - 22.21 Å. TEM observation of as-burnt powders of $SrFe_{12-2x-y}(CoZr)_xO_{19}$ shows the powder particles have an average particle size of 14-29 nm. The magnetic and electrical conductivity properties have been investigated as a function of substitution of Co and Zr ions at applied field 15 kOe. The magnetic properties have been characterized by taking into account microstructure and preferential site occupancy of sublattice sites by substituted ions. Curie temperature increases with substitution due to strong superexchange interaction. Electrical conductivity shows decreasing trend by increasing substitution. The activation energy in ferromagnetic is less than that of paramagnetic region. The change in magnetic and electrical conductivity parameters results in possible use of substituted ferrite for recording media, deflection yoke etc.

Keywords: XRD, TEM, Magnetic Properties, Electrical Properties, particle size,

1. Introduction:

M-type hexagonal strontium ferrites are known for their strong uniaxial magnetocrystalline anisotropy with easy magnetization along c-axis [1, 2]. They are being used for magnetic recording applications due to good intrinsic properties [3, 4]. These intrinsic magnetic properties, i.e saturation magnetization, residual magnetization and coercivity can be altered by cationic substitution for Fe^{3+} ions. However, it has been reported that substitution causes intrinsic coercivity to decrease effectively but at the expense of decrease in saturation magnetization, restricting the use of hexagonal ferrites for recording applications [5]. Thus increasing efforts are being made to decrease coercive force and simultaneously increasing saturation magnetization, residual magnetization. The application of hexagonal ferrites in the area of magnetic recording demands proper control of homogeneity and morphology.

In the literature, sufficient reports are available on variation of magnetic parameters of BaM ferrite with different substituents for example Co-Zr, Ni-Zr, Co-Ru, Co-Sn [6-9], etc. But magnetic behaviour of substituted Sr-ferrite, i.e. Sr-M has not been studied yet. The present work involves magnetic studies of divalent Co^{2+} ions and tetravalent Zr^{4+} ions-substituted Sr-ferrite synthesized by sol-gel combustion method.

2. Experimental:

The polycrystalline M-type hexaferrites having the following formula $SrFe_{12-2x-y}(CoZr)_xO_{19}$ (x = 0.2, 0.6, 0.8, 1.0) were prepared by sol-gel combustion starting form metal nitrates. The analytically pure materials: $Fe(NO_3)_3.9H_2O$, $Sr(NO_3)_2$, $Co(NO_3)_2$ and $Zr(NO_3)_4$ were weighed in the desired proportions and dissolved with small amounts of water. Polyvinyl alcohol was added to make a colloidal solution. The pH was adjusted (pH ~ 8) by dropping NH_4OH solution and a sol of metal hydroxides was

formed. The sol dried at 100℃ was ignited a combustion wave spontaneously propagates through the whole gel. It results a fine magnetic powder. This powder was compacted in a disc shape and the compacted samples were subjected to thermal treatment at 750℃ for 6 hrs. After each sample, the mass and dimensions of the discs were measured to determine the bulk density (d = m/V) and porosity (p = $1 - d/d_x$), where d_x is the theoretical density (X-ray density).

The X-ray powder diffraction was determined the nanometer structure of the powder obtained by combustion and was evidenced the crystallization of M-hexagonal phase by thermal treatment. The microstructure was studied by transmission electron microscopy (TEM). The particle size was determined by using formula ($D = 0.9\lambda/b\cos\theta$), where b is the percentage intensity of FWHM of XRD. The magnetic measurements were carried out by a vibrating sample magnetometer operating up to a maximum field of 15 kOe.

3. Result and Discussion:

X-ray diffraction pattern of samples (Fig. 1) show that magnetoplumbite structure has been formed. The change in relative intensities may be related to occupation of crystallographic sites by substituted ions. From structural parameters characterized by lattice constants 'a' and 'c' (Table 1), it becomes clear that lattice constant 'a' shows less variation and that of 'c' varies rapidly followed by slow variation with substitution. This is in agreement with the fact that all hexagonal ferrites exhibit constant lattice parameter 'a' and variable parameter 'c' [10]. It also indicates that change of easy magnetized c-axis is larger than a-axis with Co^{2+} and Zr^{4+} ions substitution. This is attributed to large ionic radii of Zr^{4+} ion (0.72 Å) and Co^{2+} ion (0.72 Å) than Fe^{3+} ion (0.64 Å) [7, 11].

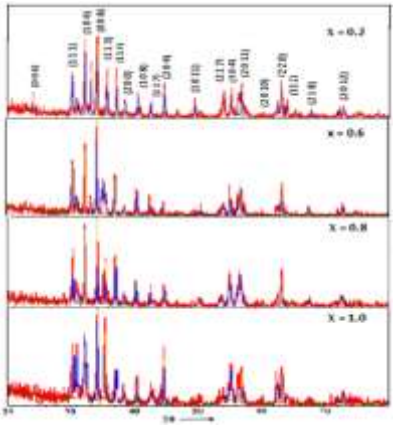

Fig. 1: X-ray diffractograms of $SrFe_{12-2x-y}(CoZr)_xO_{19}$ ferrite calcinated ad 750℃ for 6 h.

TEM (Fig. 2) shows grains of different size attributing to large ionic radii of substituted Zr^{4+} and Co^{2+} ions in comparison to Fe^{3+} ion [7, 11], thus grain size can be controlled with substitution. Grain micrograph (Fig. 2) of particles also indicates improvement in inter-grain connectivity with substitution Zr^{4+} and Co^{2+} ions. The agglomeration of grain takes place due to increase in grain size with substitution. Therefore, ferrite formation reaction is promoted by Zr^{4+} and Co^{2+} ions.

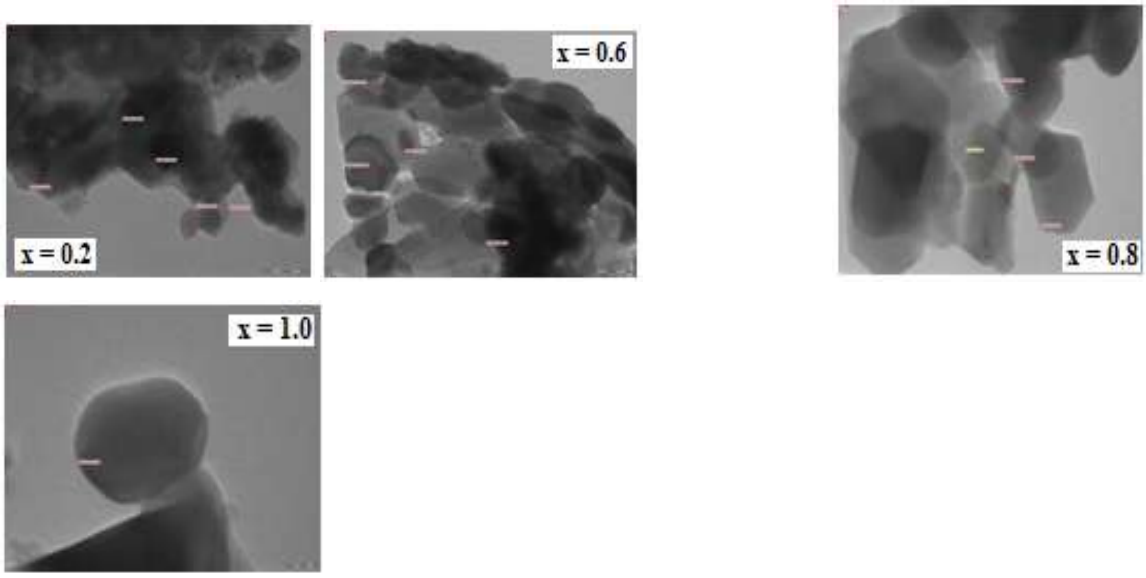

Fig. 2: TEM micrographs of $SrFe_{12-2x-y}(CoZr)_xO_{19}$ ferrite with (x = 0.2, 0.6, 0.8, 1.0)

Table-1 shows the bulk density (mass density) and x-ray density increases linearly with increase in concentration of Zr^{4+} and Co^{2+} ions but the percentage porosity (p) reduction shows the grain closeness in microstructure. Thus the number of pores is reduced, as a result of which individual grains come closer to each other and the effective area of grain to grain contact increases [12].

Electronegativity relates to attraction of valence electrons and more electronegative ions tend to occupy octahedral site. This site is larger than tetrahedral site [7]. Electronegativity for Zr and Co atoms is 1.33 and 1.88 respectively. According to Ligand theory, ions site occupancy also depends on d-configuration and nature of other participating cation [13]. In other words, Co^{2+} ions prefer to occupy octahedral site with d^7 configuration and Zr^{4+} ions have no site preference owing to d^0 configuration. Also Zr^{4+} ions ($4p^6$ configuration) are less compressible than Co^{2+} ions ($3d^7$ configuration), therefore presumably occupy octahedral site. It has been reported that Co^{2+} ions have preferential occupancy of 4fI-4fII site [14]. Zr^{4+} ions shows preference to occupy both tetrahedral, octahedral sites for lower substitution an octahedral site for higher substitution [7], and Li at el. reported the occupancy of Co-Zr ions on 12k and 2b sites [6].

Table-1: Lattice constants a and c, X-ray density, bulk density, porosity, particle size, Curie temperature of $SrFe_{12-2x-y}(CoZr)_xO_{19}$ ferrite.

Substitution (x)	a (Å)	c (Å)	X-ray density (d_x) = 2M/NV (gm/cm³)	Bulk density (d)= m/v (gm/cm³)	Porosity (p)= 1-(d/ d_x)	Particle size, D = 0.9λ/(hcosθ) (nm)	Curie Temp. Tc (℃)
0.2	5.8088	22.083	5.506	4.3638	0.2074	19.5872	413
0.6	5.8505	22.1272	5.495	5.0224	0.0860	23.62	433
0.8	5.8526	22.1936	5.513	5.0665	0.0809	29.5154	442
1.0	5.8625	22.2168	5.528	5.1208	0.0736	14.7606	463

The curves of hysteresis loop [Fig. 3 (a) & (b)] show that sample exhibit sharp increase in magnetization at low applied field, which slows

down at high field. This is a typical behaviour of multidomain particles [15], microstructure (Fig. 2) also exhibits multidomain behaviour. There is fall in slope with substitution of Zr^{4+} and Co^{2+} ions and sample 1.0 nearly attains more saturated state than that of sample 0.2 substitutions.

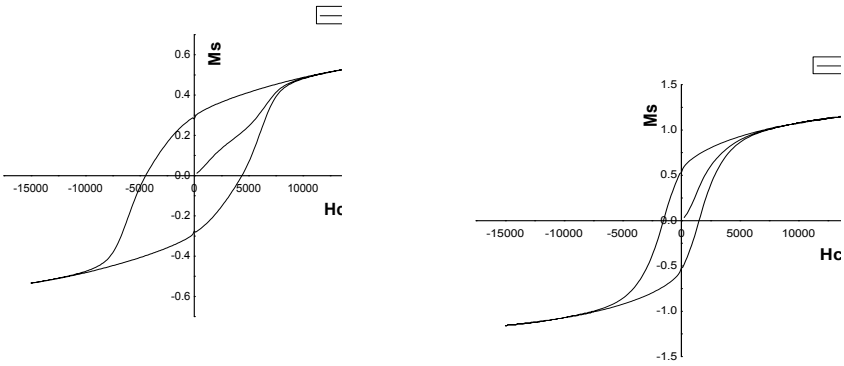

(a) **(b)**

Fig. 3[(a), (b)]: Hysteresis graphs of $SrFe_{12-2x-y}(CoZr)_xO_{19}$ ferrite with (x = 0.2, 1.0) at room temperature.

In M-type hexagonal ferrite, Fe^{3+} ions occupy seven octahedral sites 12k and 2a, trigonal site 2b with spins in one direction, two octahedral sites 4fI and two tetrahedral sites 4fII with spins in opposite directions. The variation of magnetic properties with substitution x = 0.2 and 1.0 shown in Fig. 3 (a) & (b). The sample with x = 0.2 doping exhibits high coersivity which is due to uniaxial magnetocrystalline anisotropy along c-axis. Coercivity rapidly falls with substitution of Zr^{4+} and Co^{2+} ions at x = 0.2 to 1.0. This fast reduction in coercivity is primarily related to intrinsic effect associated with replacement of Fe^{3+} ions at 4fII and 2b sites.

Another reason for reduction in coercivity is extrinsic effect which causes increase in grain size with substitution. TEM morphology (Fig. 2) also depicts same variation. This effect is authenticated by the fact that coercivity is inversely related to grain size [16]. Furthermore,

microstructure shows more intergranular pores in sample with x = 0.2 doping. These pores offer hindrance to the flow of applied field across the grains. The grain size increment with substitution reduces intergranular pores. Therefore, ferrite can be demagnetized at low applied field, which decreases coercivity. This also affirms that porosity strongly affects coercivity [17]. Pores act as non-magnetic inclusions and discourage grains connectivity. More specifically, Zr^{4+} and Co^{2+} ions substitution cause change of easy axis of magnetization from c-axis to basal plane. Fast reduction of coercivity (H_c) occurs by 67.5% from sample x = 0.2 (4500 Oe) to x = 1.0 (1500 Oe) and the same decrease by 25% in Ba-Co-Zr ferrite [6].

Magnetization variation is related to distribution of substituents on five crystallographic sites, i.e. 12k-2a-2b (spin-up) and 4fI-4fII (spin-down). The substitution of Fe^{3+} ions in spin-up state reduces magnetization and it increases with substitutions on spin-down state.

Saturation magnetization (Ms) and retentivity (Mr) increases [Fig. 3 (a) & (b)] with substitution of Zr^{4+} and Co^{2+} ions from x = 0.2 to 1.0 shown in Table-2. This can be ascribed to replacement of Fe^{3+} ions (causing saturation magnetization reduction) in spin-down state by Zr^{4+} and Co^{2+} ions. Also it has been reported that saturation magnetization increases and retentivity with substitution of Fe^{3+} ions by non-magnetic ions [18]. However, Ms and Mr increases at higher substitution attributing to the fact that the magnetic moments of both ions are not able to cancel out with spin-down moment of Fe^{3+} ions ($5\mu_B$) owing to weak magnetic nature of Co^{2+} ions ($3\mu_B$) and diamagnetic Zr^{4+} ions ($0\mu_B$). More specifically, weakening of superexchange interaction (Fe_A^{3+} -O-Fe_B^{3+}) will collapse magnetic collinearity with substitution with substitution of Zr^{4+} and Co^{2+} ions. This is confirmed from measured values of Curie temperature. Table-1 shows increase in Curie temperature from 413℃ to 463℃ with substitution.

Table-2:

Saturation magnetization (Ms), Retentivity (Mr) and Coercivity (Hc) of $SrFe_{12-2x-y}(CoZr)_xO_{19}$ ferrite.

substitution (x)	Ms(emu/gm)	Mr (emu/gm)	Hc (Oe)
0.2	25.619	13.381	4500
1.0	48.75	22.042	1500

When compared with other substitutions, Ni-Zr [7], Co-Ru [8], Co-Sn [9], Sn-Ru [19], Co-Ti [20], etc., it becomes clear that Zr^{4+} and Co^{2+} ions enhance Ms and Mr and decrease Hc better than the above reported substitution.

The X-ray density has been calculated using the relation for hexagonal ferrites [21]

$$dx = \frac{2M}{N\ 0.866a^2c}$$

where, M represents the molecular weight of the sample, 'a' and 'c' are the lattice parameters of the hexaferrite samples and N the Avogadro's number. The X-ray density (dx) depends on the lattice constant and molecular weight of the sample whereas the bulk density (d) of the sample can be calculated from the geometry of the crystals and mass of the samples. Both the densities (dx and d) as functions of Co-Zr concentrations are depicted in Table-1. The decrease in porosity with the increase in concentration of Co and Zr which increases the grain to grain contact, it increases the strength of material having more decisive the material. Further, strength of the given material is mainly governed by the strength of cation-cation bonding rather than strength of cation-anion bonding in the system. This depends on the specific gravity of the Co^{2+} and Zr^{4+} ions.

Logarithmic electrical conductivity versus inverse temperature plot has been found to be linear with a kink to the Curie temperature as shown in Fig. 4 (a), (b), (c). The room temperature resistivity increases as

the concentration of Co-Zr increases and that of Fe^{3+} decreases. This implies that the room temperature conductivity decreases. The activation energy has been found to be in the range of 0.47 to 0.67 eV in paramagnetic region and 0.35 to 0.38 eV in ferromagnetic region. All these parameters are depicted in Table-3. In the paramagnetic region, the activation energy increases than that of ferromagnetic region because of valence exchange mechanism between Fe^{3+} and Fe^{2+} ions [22]. The Curie temperature (Tc) calculated from magnetic measurements and transition temperature (Tt) calculated from electrical measurements. Both these temperatures have been found to be analogous to each other.

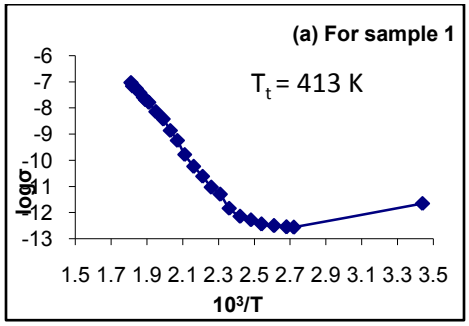

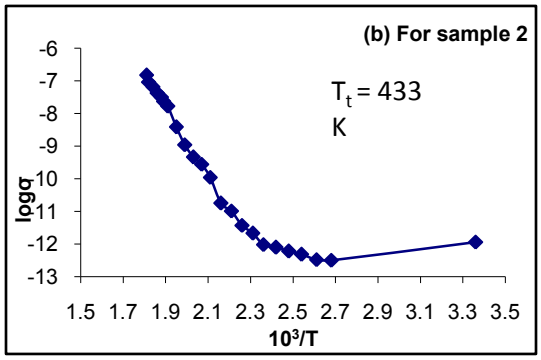

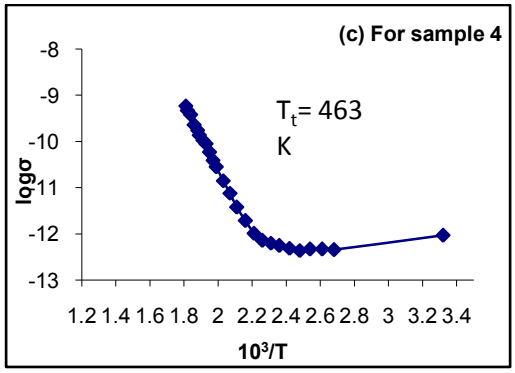

Fig. 4(a),(b),(c): Electrical conductivity curves of $SrFe_{12-2x-y}(CoZr)_xO_{19}$ ferrite with (x = 0.2, 0.6 and 1.0).

Table-3:

Activation energy, room temp. resistivity and conductivity, transition temp. of $SrFe_{12-2x-y}(CoZr)_xO_{19}$ ferrite.

Conc. x $Sr(CoZr)_xFe_{12-2x-y}O_{19}$	Activation Energy		Resistivity at Room temp. Ω-m	Conductivity at room temp. S/m	Transition temp T_t(℃)
	Ferri. (eV)	Para. (eV)			
0.2	0.357	0.625	$1.148x10^5$	$8.708x10^{-6}$	413
0.6	0.365	0.657	$1.527x10^5$	$6.548x10^{-6}$	433
0.8	0.36	0.675	$1.601x10^5$	$6.244x10^{-6}$	442
1	0.383	0.471	$1.673x10^5$	$5.975x10^{-6}$	463

Conclusions:

XRD studies of the samples showed hexagonal magnetoplumbite (M) structure with unit cell dimensions 'a' and 'c' varies from 5-6 Å and 21-23 Å. The mass density of the ferrites has been found to vary linearly and depend upon the samples mass and volume. The X-ray density also varies linearly and depends upon the lattice constant and molecular weight of the sample. The computation of porosity has been done by bulk and X-ray density of the studied samples. The TEM morphology and XRD analysis revealed that the concluded size of the molecules of the studied samples is hexagonal in shape. The calculated value of the particle size of the atom varies in the range of 14-29 nm which is shown in Table-1. VSM studies of the samples shows that the increase in saturation magnetization and retentivity and decrease in coercivity as the increase Co-Zr concentration. Electrical conductivity decreases as the increasing conc. of Co-Zr. The activation energy has been found in the range of 0.47 to 0.67 eV in paramagnetic region and 0.35 to 0.38 eV in ferromagnetic region.

References :

Y. Li, R. Liu, Z. Zhang, C. Xiong. (2000). Mater Chem. Phys. 64, 256-259.

J.H. Choy, Y.S. Han, S.W. Song. (1994). Mater. Lett 19, 257-262.

D. E. Speliotis, (1989). IEEE Trans. Magn. 25, 4048-4050.

R.G. Simmons, (1989). IEEE Trans. Magn. 25, 4051-4053.

Q. Fang, H. Cheng, K. Huang. J. Wang, R. Li, Y. Jiao, (2005). J. Magn. Magn. Mater. 294, 281-286.

Z.W. Li, L. Chen, C. K. Ong. (2002). J. Appl. Phys. 92, 3902-3907.

M.V. Rane, D. Bahur, S.D. Kulkarni, S.K. Date, (1999). J. Magn. Magn. Mater. 195, L256-L260.

H.S. Cho, S.S. Kim, (1999). IEEE Trans. Magn. 35, 3151-3153.

D. Lisjak, M. Drofenik, (2004). J. Eur. Cer. Soc. 24, 1841-1845.

H. Kojima, in: E.P. Wohlfarth (Ed.), (1982). Ferromagnetic Materials, vol. 3, North-Halland, Amsterdam, 305 pp.

T.M. Meaz, C.B. Koch, (2004). Hyp. Interact. 156/157, 341-346.

M.K. Moinuddin and S.R. Murthy, (1993). J. Alloys Compound, 194, 105.

M.V.Rane, D. Bahadur, A.K. Nigam, C.M Shrivastva, D. Kulkarni, S.K. Date, (1999). J. Magn. Magn. Mater. 192, 288-296.

Z. Simsa, S. Lego, R. Gerber, E. Pollert, (1995). J. Magn. Magn. Mater. 140-144, 2103-2104.

U. Topal, H. Ozkan, H. Sozeri, (2004). J. Magn. Magn. Mater. 284, 416-422.

J. Dho, E.K. Lee,J.Y. Park, N.H. Hur, (2005). J. Magn. Magn. Mater. 285, 164-168.

H.P.J. Wijn, E.W. Gorter, C.J. Esveldt, P. Geldermans, (1954). Philips Tech. Rev. 16, 49-58.

H.C. Fang, Z. Yang, C.K. Ong, y. Li, C.S. Wang, (2002). J. Magn. Magn. Mater. 242-245, 430-433.

A. Gonsalez-Angeles, G. Mendoza-Suarez, A. Gruskova, J. Slama, J. Lipka, M. Papanova, (2005). Mater. Lett. 59, 1815-1819.

X.Z. Zhou, A.H. Morrish, Z.W. Li, Y.K. Hong, (1991). IEEE Trans. Magn. 27, 4654-4656.

M.U. Iskan, I. Ahmad, T. Abbas, (1999). Porceedings of the Sixth International Symposium on Advanced Materials, 155-p.

K. Heneda, H. Kojima, (1971). Physica Status Solidi (A). 6, 256-p.